

# A Two-Dimensional Thermal Analysis of a New High-Performance Tubular Solar Collector

F. L. Lansing and C. S. Yung  
DSN Engineering Section

*This article is the first of two which describe and analyze the thermal performance of the new General Electric vacuum tube solar collector. The assumptions and mathematical modeling are presented. The problem is reduced to the formulation of two simultaneous linear differential equations characterizing the collector thermal behavior. After applying the boundary conditions, a general solution is obtained which is found similar to the general Hottel, Whillier and Bliss form but with a complex flow factor.*

## I. Introduction

Several solar-powered heating and cooling facility modifications in the Deep Space Network ground stations are planned for future implementation as part of the DSN Energy Conservation Project. In order to support the relevant feasibility and advanced engineering studies, special attention is given to new technologies in low-concentration, nontracking solar collectors. These nonimaging low-concentration types (with intensity concentration between 1 and 5) possess several advantages compared to the high-temperature, high-concentration ones. Examples are:

- (1) The ability to harness, diffuse and direct portions of sunlight.
- (2) Low cost due to less precision requirements in manufacturing, no sun-tracking mechanisms and no sophisticated optics controls.
- (3) Good collection efficiency in the range of heating/cooling interest from 80 to 140°C.

One of the new designs that emerged in this field is the tubular and evacuated collector manufactured by General

Electric (Ref. 1). The collector resembles, but is not identical to, a hybrid system combining (1) the serpentine tube on a flat absorber enclosed in an evacuated glass cylinder manufactured by Corning Glass Works, and (2) the all-glass concentric tubes manufactured by Owens-Illinois (Refs. 2-4). The semiproprietary GE collector performance data given by the manufacturer claim that the collector is able to provide about double the energy collection capability of flat plate collectors employing double glazing and selective coating. Although the GE collector does possess the best of each of the Owens-Illinois and the Corning types, it is felt that its performance superiority is in need of an in-depth investigation at a wide range of operating conditions. This article, the first of two, is intended to provide the collector thermal analysis and the relevant equations needed for a full parameterization study.

## II. Collector Description

Figure 1 illustrates the design details of one module of the tubular collector with 10 heat collection units. The units are mounted in parallel and each unit contains, as shown in Fig. 2, a U-shaped copper tube. The copper tubes of the units are connected in series to form a serpentine of 10 loops.

Each collector unit consists of two coaxial glass tubes. The annular space between the glass tubes is evacuated and sealed to form a "thermos-bottle" effect. A thin cylindrical shell made of copper conforms to the inside diameter of the inner glass tube and is attached to the copper U-tube. The vacuum tubes are mounted in a polished aluminum V-shaped back reflector tray. The back reflector enhances the solar concentration and allows both direct and diffuse portions of the sunlight to be collected.

The solar collector manufactured by General Electric has a selective coating on the outer surface of the inner glass tube, thus making the inner glass tube serve as the absorber that transmits heat to the copper shell by conduction. Since glass is a poor conductor compared to copper, the present collector under study is made differently and more efficient by selectively coating the outer surface of the copper shell instead, while keeping the inner glass tube transparent. Accordingly, the double-walled glass bottle serves as the window and the thin copper shell with its selective outer surface acts as the absorber.

Besides employing (1) a vacuum technique to reduce convection losses, (2) a selective coating to reduce outward infrared radiation losses, and (3) a back augmenting reflector, the collector has unique features compared to other commercial tubular collectors. Examples are (1) a glass tube which, if damaged, will not discontinue the collector service, and (2) the collector is lightweight with a low thermal inertia which can be translated to ease in installation, connection and structural requirement plus a fast temperature response that increases a full-day performance.

### III. Thermal Analysis

Before we proceed with the analytical energy expression for each collector tube in a collector unit, the following assumptions were made to simplify the simulation process.

- (1) The collector is assumed at steady state, located in an environment with uniform ambient temperature and solar irradiation.
- (2) The problem is treated as a two-dimensional heat transfer in the axial and radial directions. Collector tubes are assumed to be of uniform temperature in the tangential direction, even though the solar flux distribution on the outer glass tube may not be uniform due to the space allowed between the collector units and the effect of the back V-reflector. In the radial direction, the temperature distribution is assumed to be in steps with negligible conduction thermal resistance for all thin tubes.
- (3) Axial conduction heat transfer from one end to another is neglected.
- (4) Material optical properties are assumed uniform and independent of temperature and direction. Physical properties for solids and liquids are also assumed uniform and independent of working temperature and pressure.
- (5) Sky and ambient temperatures are assumed approximately the same to simplify computations. Also, the ambient air temperature to the air core and external to the collector unit is assumed the same.
- (6) The metallic absorber shell, the hot water tube wall and the cold water tube wall are all assumed at a single temperature, which is the average of these three surfaces. The absorber temperature varies only axially. The metallic absorber actually acts as a fin stretched from both sides of the fluid tubes in a circular shape. This assumption is supported by the observation that the difference in temperature between inlet and outlet fluids is small at each collector unit.
- (7) The convective heat transfer coefficient between the serpentine tube and either the hot or cold fluid sides is assumed the same since its variation with temperature is insignificant. The convective coefficient is a dominant function of tube diameter length and fluid mass flow in the laminar range.

A segment of the collector unit whose thickness is  $dx$  and located at a distance  $x$  from the open end of the fluid tubes is analyzed. Appendix A gives the effective optical properties of the double concentric glass cylinders. In Appendix B, the details of the heat balance equations are given for reference. The collector and thermal behavior is characterized by the following two linear simultaneous differential equations for the hot fluid temperature  $T_h(x)$  and the cold fluid temperature  $T_c(x)$ :

$$\frac{dT_h}{dx} = -\delta - C_0 T_c + C_1 T_h \quad (1)$$

$$\frac{dT_c}{dx} = \delta + C_0 T_h - C_1 T_c \quad (2)$$

where  $\delta$ ,  $C_0$  and  $C_1$  are collector characteristic constants given in Appendix B. If Eqs. (1) and (2) are solved for either  $T_c$  or  $T_h$  alone, then

$$\left. \begin{aligned} \frac{d^2 T_c}{dx^2} - (C_1^2 - C_0^2) T_c + \delta (C_1 + C_0) &= 0 \\ \frac{d^2 T_h}{dx^2} - (C_1^2 - C_0^2) T_h + \delta (C_1 + C_0) &= 0 \end{aligned} \right\} \quad (3)$$

The general solution for Eq. (3) can be written after substitution in Eqs. (1) and (2) to be in the form

$$T_c(x) = Y_1 \exp(nx) + Y_2 \exp(-nx) + \frac{\delta}{(C_1 - C_0)} \quad (4)$$

$$T_h(x) = \left( \frac{C_1 + n}{C_0} \right) Y_1 \exp(nx) + \left( \frac{C_1 - n}{C_0} \right) Y_2 \exp(-nx) + \frac{\delta}{(C_1 - C_0)} \quad (5)$$

where  $Y_1$  and  $Y_2$  are arbitrary constants to be determined from the boundary conditions, and  $n$  is determined from

$$n = \sqrt{C_1^2 - C_0^2} \quad (6)$$

#### IV. Boundary Conditions

Equations (4) and (5) are subject to the following two boundary conditions:

- (1) At the inlet fluid section ( $X=0$ ), the cold fluid temperature  $T_c(0)$  is given.
- (2) At the closed end section ( $X=L$ ), the cold fluid temperature is equal to the hot fluid temperature.

Substituting in Eqs. (4) and (5), the temperature distribution  $T_c(x)$  and  $T_h(x)$  is given by

$$T_c(x) = \frac{\delta}{(C_1 - C_0)} - \left[ \frac{\delta}{(C_1 - C_0)} - T_c(0) \right] \left[ \frac{n \cosh n(L-x) + (C_1 - C_0) \sinh n(L-x)}{n \cosh nL + (C_1 - C_0) \sinh nL} \right] \quad (7)$$

$$T_h(x) = \frac{\delta}{(C_1 - C_0)} - \left[ \frac{\delta}{(C_1 - C_0)} - T_c(0) \right] \left[ \frac{n \cosh n(L-x) - (C_1 - C_0) \sinh n(L-x)}{n \cosh nL + (C_1 - C_0) \sinh nL} \right] \quad (8)$$

#### V. General Findings

##### A. The Flow Factor ( $F$ )

The temperature difference between cold and hot fluids at any location ( $x$ ) is given from Eqs. (7) and (8) by

$$[T_h(x) - T_c(x)] = \left[ \frac{\delta}{(C_1 - C_0)} - T_c(0) \right] \left[ \frac{2(C_1 - C_0) \sinh n(L-x)}{n \cosh nL + (C_1 - C_0) \sinh nL} \right] \quad (9)$$

Particularly, at the open end ( $x=0$ ), both the temperature difference and the net heat collected per unit collector area are determined using Eq. (9) as

$$[T_h(0) - T_c(0)] = \left[ \frac{\delta}{(C_1 - C_0)} - T_c(0) \right] \left[ \frac{2(C_1 - C_0) \sinh nL}{n \cosh nL + (C_1 - C_0) \sinh nL} \right] \quad (10)$$

and

$$Q''_{coll} = \frac{\dot{m}c_p}{SL} [T_h(0) - T_c(0)] \quad (11)$$

where  $S$  is the spacing between any two collector units.

Using the conductance coefficients ( $B$ 's) defined in Appendix B, the extracted energy by the fluid is rewritten as

$$Q''_{coll} = \underbrace{\left[ E_1 + E_2 \frac{B_4}{B_7} + E_3 \frac{B_6}{B_7} \right]}_{\text{Energy absorbed}} - \underbrace{B_0 (T_c(0) - T_A)}_{\text{Energy lost to ambient air}} \cdot F \quad (12)$$

where  $F$  is a dimensionless "flow-factor" defined by

$$F = \frac{GD_{f,0}}{SL B_0} \left[ \frac{2 \sinh nL}{\left(\frac{B_3}{nG}\right) \cosh nL + \sinh nL} \right] \quad (13)$$

where  $B_0$  is the overall heat transfer coefficient given by Eq. B-25. If the collector glass tubes were made such that the glass absorptivity  $\alpha_{f,e}$  and  $\alpha_{s,e}$  are negligible, Eq. (12) will become similar to the general Hottel, Whillier and Bliss form

$$Q''_{coll} \cong \{E_1 - B_0 [T_c(0) - T_A]\} \cdot F$$

## B. Collector Efficiency

The collector efficiency based on the solar radiancy on the projected area is defined by

$$\eta = \frac{Q''_{coll}}{I}$$

or, using Eq. (12),

$$\eta = F \left\{ \lambda \left[ \alpha_{a,e} + \alpha_{f,e} \frac{B_4}{B_7} + \alpha_{s,e} \frac{B_6}{B_7} \right] - B_0 \frac{[T_c(0) - T_A]}{I} \right\} \quad (14)$$

Equation (14) suggests that if the collector efficiency is plotted vs  $(T_c(0) - T_A)/I$ , the results would fit approximately

a straight line whose slope ( $B_0 F$ ) is an indication of the heat losses to the ambient and the intercept is an indication of the optical characteristics.

## C. Highest Temperature at "No-Flow"

The temperature of the collector with "no-flow" or stagnant condition is an important value needed for coating stability and temperature control. Setting the temperature difference  $[T_h(0) - T_c(0)]$  from Eq. (10) to the limit as  $G$  approaches zero (or  $n$  approaches  $\infty$ ) one can prove that

$$\begin{aligned} \text{Limit}_{\text{as } n \rightarrow \infty} [T_h(0) - T_c(0)] = & \\ & \frac{2 \left[ \left( E_1 + E_2 \frac{B_4}{B_7} + E_3 \frac{B_6}{B_7} \right) - (T_c(0) - T_A) \right]}{B_0 \left[ 1 + \sqrt{1 + (2 \bar{B}_3/B_0)} \right]} \end{aligned} \quad (15)$$

where  $\bar{B}_3$  is the free-convection heat transfer coefficient between absorber tubes and fluid. If the collector was left with a very small flow rate under the sun with an inlet temperature equal to ambient temperature  $T_A$ , the simulated maximum temperature of the leaving fluid will be

$$T_{h_{max}}(0) \cong T_A + \frac{E_1}{B_0} \cdot \frac{2}{1 + \sqrt{(2 \bar{B}_3/B_0) + 1}} \quad (16)$$

To support the parameterization study and the numerical evaluation of the above findings, a short computer program is written using the optical properties of Appendix A, the heat balance equations of Appendix B, and the temperature distribution given by Eqs. (7) and (8). The results of the second phase of this study will be the subject of the second report.

## References

1. General Electric Solartron Model TC100 Vacuum Tube Solar Collector Publication, General Electric, Space Div., Phil., Pa.
2. Lansing, F. L., "Heat Transfer Criteria of a Tubular Solar Collector – The Effect of Reversing the Flow Pattern on Collector Performance," in *The Deep Space Network Progress Report 42-31*, pp. 108-114, Jet Propulsion Laboratory, Pasadena, Calif., Feb. 1976.
3. Lansing, F. L., *The Transient Thermal Response of a Tubular Solar Collector*, Technical Memorandum 33-781, NASA, July 1976.
4. Lansing, F. L., "A Two-Dimensional Finite Difference Solution for the Transient Thermal Behaviour of a Tubular Solar Collector," in *The Deep Space Network Progress Report 42-35*, pp. 110-127, Jet Propulsion Laboratory, Pasadena, Calif., Oct. 1976.
5. Kreith, F., *Principles of Heat Transfer*, Second Edition, Intext Educational Publishers, New York, 1968.
6. Duffie, J. A., and Beckman, W. A., *Solar Energy Thermal Process*, Wiley Interscience Publication, New York, 1974.

## Definitions of Terms

$a$	glass absorption coefficient	$Y$	constants, K
$b$	absorber reflection coefficient	$\alpha$	absorptivity
$B_0 \rightarrow B_8$	thermal conductance, kW/m <sup>2</sup> °C	$\rho$	reflectivity
$C_p$	fluid specific heat, kWh/kg°C	$\tau$	transmissivity
$C_0, C_1$	constants	$\lambda$	augmented radiation factor
$D$	diameter	$\eta$	collector efficiency
$E_1 \rightarrow E_6$	energy flux, kW/m <sup>2</sup>	$\delta$	parameter, °C/m
$F$	flow factor	$\epsilon$	emissivity
$G$	heat capacity = $\dot{m}C_p/D_{f,o}$		
$H$	convective heat transfer coefficient, kW/m <sup>2</sup> °C	Subscripts	
$I$	solar flux kW/m <sup>2</sup>	$A$	air in collector core
$K$	thermal conductivity, kW/m°C	$Am$	ambient air
$L$	collector-unit length, m	$a$	absorber shell
$\dot{m}$	fluid mass flow rate, kg/h	$c$	cold fluid
$n$	characteristic constant, m <sup>-1</sup>	$e$	effective
$Q$	heat rate, kW	$f$	first (outer) glass tube
$r$	glass reflection coefficient	$h$	hot fluid
$R$	equivalent radiation heat transfer coefficient, kW/m <sup>2</sup> °C	$i$	inside
$S$	spacing between two consecutive collector units, m	$o$	outside
$T$	temperature, K	$s$	second (inner) glass tube
$X$	distance	$t$	serpentine tube
		$\nu$	V-shaped reflector

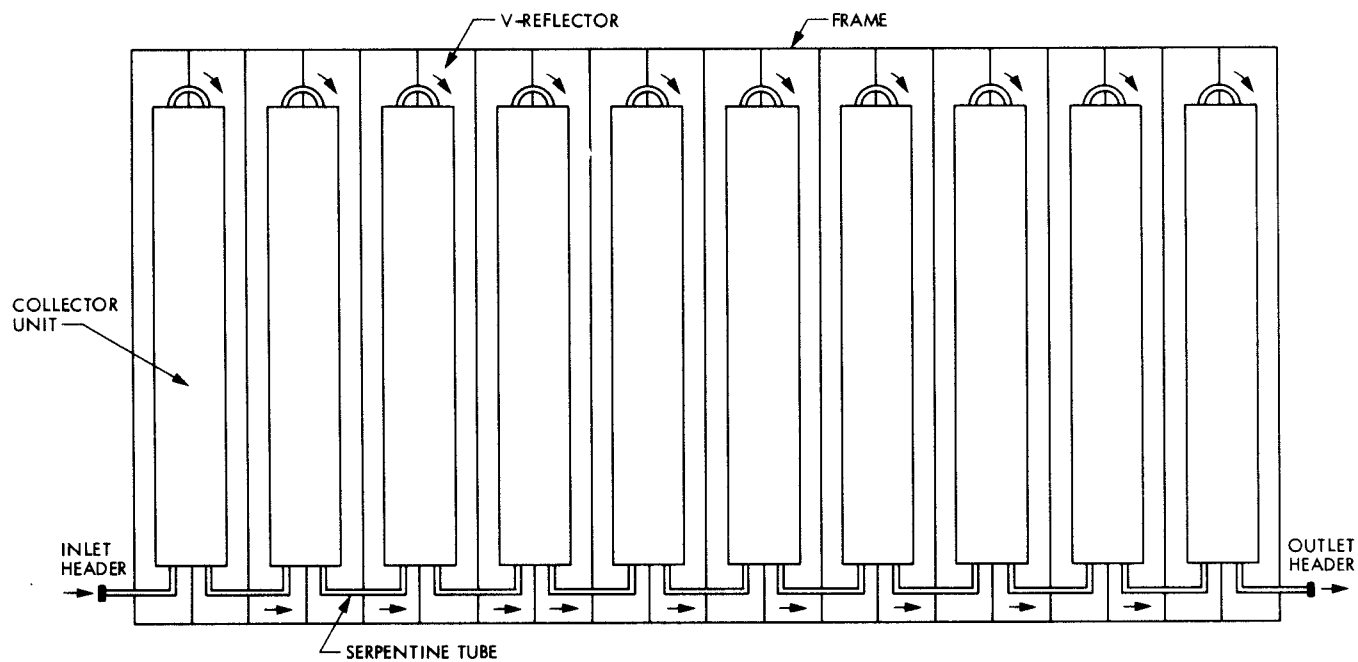


Fig. 1. A single collector module composed of 10 units

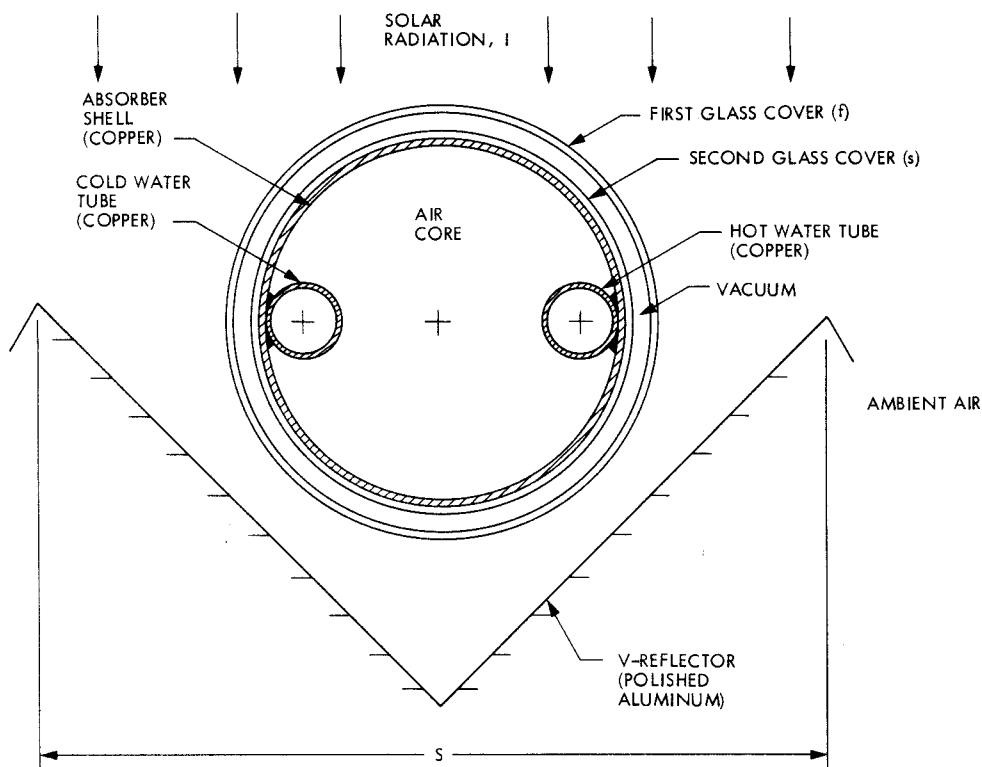
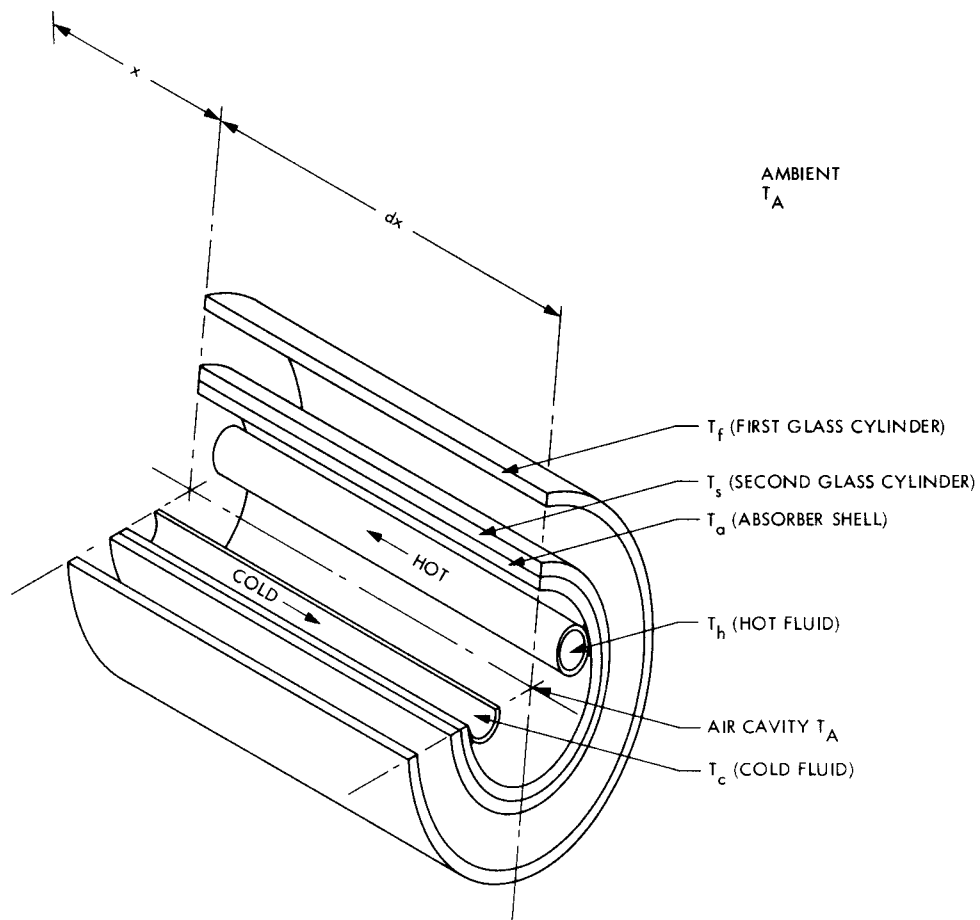


Fig. 2. Collector unit



**Fig. 3. Segment of a collector unit with thickness  $dx$**



## Appendix A

### Derivation of Optical Properties

In this appendix the effect of multiple reflections, absorption, and refraction of direct solar rays incident upon the collector tubes is discussed. The derivation of the effective absorptivity, reflectivity, and transmissivity will be made for each of the exterior glass tubes, the interior glass tube and the metallic absorber shell.

Since the radial spacing between the two coaxial glass tubes is small compared to their diameter, the optical properties derivation will be carried out assuming two parallel glass plates instead.

#### A-1. Optical Properties of a Single See-Through Sheet of Glazing

Figure A-1 shows the paths of a single beam of light when it falls on a single see-through sheet of glass. The intensity is assumed unity since the optical properties are dimensionless. The coefficients of absorption  $a$  and reflection  $r$  are applied both to the top and the bottom surfaces of the single glazing. The net transmissivity of a single glazing will be given by

$$\tau_f = a(1-r)^2 + a^3r^2(1-r)^2 + a^5r^4(1-r)^2 + \dots$$

Using the infinite geometric series sum,  $\tau_f$  is written as

$$\tau_f = \frac{a(1-r)^2}{1-a^2r^2} \quad (\text{A-1})$$

Similarly, the absorptivity  $\alpha_f$  is written as

$$\alpha_f = (1-a)(1-r) + ar(1-a)(1-r) + a^2r^2(1-a)(1-r) + \dots$$

or

$$\alpha_f = \frac{(1-r)(1-a)}{1-ra} \quad (\text{A-2})$$

Since the first law of thermodynamics states that

$$\alpha_f + \tau_f + \rho_f = 1$$

then, the reflectivity  $\rho_f$  can be expressed as

$$\rho_f = r + \frac{ra^2(1-r)^2}{1-r^2a^2} \quad (\text{A-3})$$

The above optical properties are given the subscript  $f$  since they represent the properties of the first (outer) glass tube of the collector unit.

#### A-2. Optical Properties of a Single Sheet of Glazing with Opaque Bottom Surface

Figure A-2 illustrates the paths of a single light beam on a single sheet of glass whose bottom surface is opaque. The optical properties for this glazing type will be given a subscript  $S$  since it represents the second (inner) glass tube that surrounds the metallic absorber shell. In this case, the reflection coefficient  $r$  at the top surface and that at the bottom opaque surface  $b$  will be different. The absorption coefficient  $a$  will be the same as in case A-1, if all glazings have the same thickness and material. The optical properties can be obtained by summing the infinite geometric series of intensity taken from Fig. A-2. Accordingly, for the bottom surface

$$\alpha_B = a(1-r)(1-b) + a^3br(1-r)(1-b) + a^5b^2r^2(1-r)(1-b) + \dots$$

or

$$\alpha_B = \frac{a(1-b)(1-r)}{1-a^2br} \quad (\text{A-4})$$

Also,

$$\alpha_S = (1-r)(1-a) + ab(1-a)(1-r) + a^2br(1-r)(1-a) + \dots$$

$$\alpha_S = \frac{(1-r)(1-a)(1+ab)}{1-a^2br} \quad (\text{A-5})$$

Since the energy conservation law can be written as

$$\alpha_B + \alpha_S + \rho_S = 1$$

then one can prove that

$$\rho_S = r + \frac{a^2 b (1-r)^2}{1 - a^2 b r} \quad (\text{A-6})$$

or

$$\alpha_{f,e} = \alpha_f + \frac{\alpha_f \tau_f \rho_S}{1 - \rho_f \rho_S} \quad (\text{A-8})$$

Similarly, for the second glazing, the effective absorptivity  $\alpha_{S,e}$  is expressed as:

$$\alpha_{S,e} = \alpha_S \tau_f + \alpha_S \tau_f \rho_f \rho_S + \alpha_S \tau_f \rho_f^2 \rho_S^2 + \dots$$

or

$$\alpha_{S,e} = \frac{\alpha_S \tau_f}{1 - \rho_f \rho_S} \quad (\text{A-9})$$

On the other hand, the sum of reflections from the first glazing will be written as:

$$\rho_{f,e} = \rho_f + \rho_S \tau_f^2 + \rho_f \rho_S^2 \tau_f^2 + \rho_f^2 \rho_S^3 \tau_f^2 + \dots$$

or

$$\rho_{f,e} = \rho_f + \frac{\rho_S \tau_f^2}{1 - \rho_f \rho_S} \quad (\text{A-10})$$

Equations (A-7) through (A-10) are the effective properties to be used for the thermal analysis. As a cross-checking, the properties also satisfy the energy conservation law where

$$\alpha_{f,e} + \alpha_{s,e} + \alpha_{a,e} + \rho_{f,e} = 1 \quad (\text{A-11})$$

### A-3. Combining Two Sheets of Glazing With an Opaque Bottom Surface for the Second Sheet

Combining the above two separate cases in Sections A-1 and A-2, the effective optical properties of each glazing will be derived using the light paths as illustrated in Fig. A-3. The properties of the first glazing will be  $\tau_f$ ,  $\alpha_f$ , and  $\rho_f$  as expressed by Eqs. (A-1), (A-2), and (A-3), respectively. For the second glazing, the properties  $\alpha_B$ ,  $\alpha_S$ , and  $\rho_S$  are given by Eqs. (A-4), (A-5), and (A-6), respectively. The effective absorptivity  $\alpha_{a,e}$  of the metallic absorber shell surface next to the second glazing will be found by summing the infinite series.

$$\alpha_{a,e} = \alpha_B \tau_f + \alpha_B \tau_f \rho_f \rho_S + \alpha_B \tau_f \rho_f^2 \rho_S^2 + \dots$$

or

$$\alpha_{a,e} = \frac{\alpha_B \tau_f}{1 - \rho_f \rho_S} \quad (\text{A-7})$$

Also, the effective absorptivity of the first glazing  $\alpha_{f,e}$  when it is placed next to the second glazing is determined by summing the infinite series

$$\alpha_{f,e} = \alpha_f + \alpha_f \tau_f \rho_S + \alpha_f \tau_f \rho_f \rho_S^2 + \alpha_f \tau_f \rho_f^2 \rho_S^3 + \dots$$

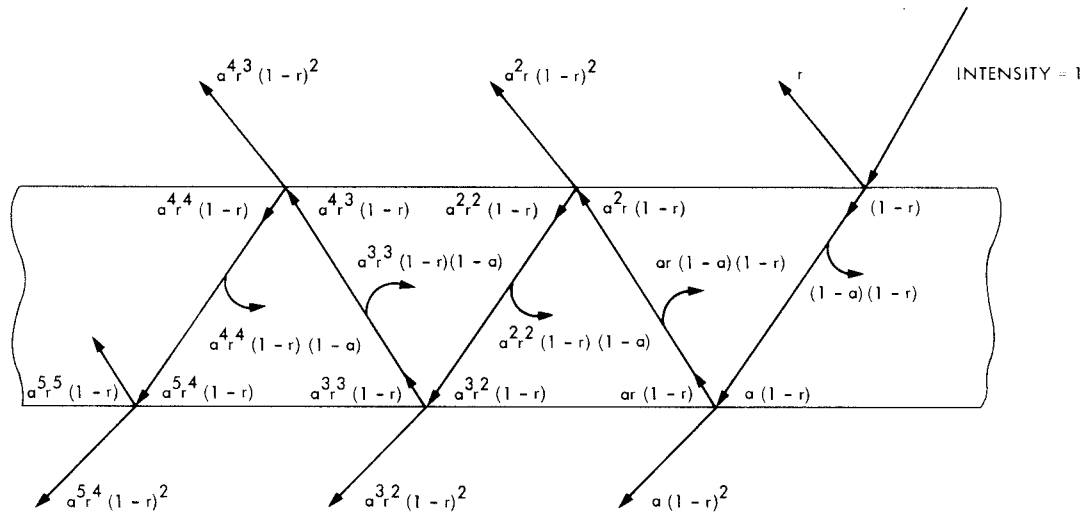


Fig. A-1. Paths and intensities of a light beam on a single glazing

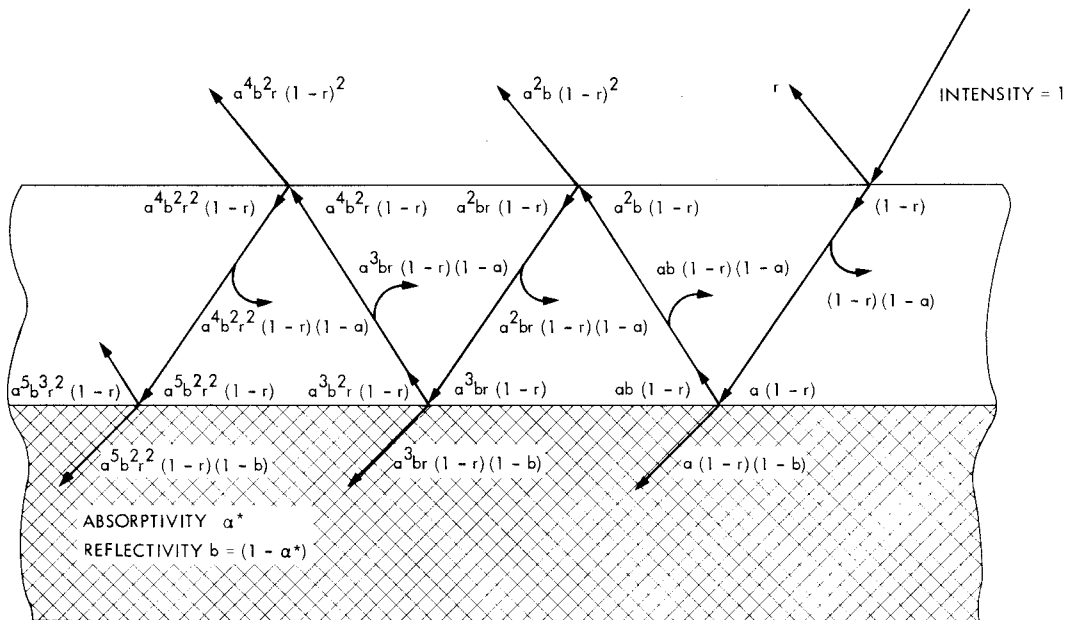


Fig. A-2. Paths and intensities of a light beam on a single glazing with opaque bottom surface

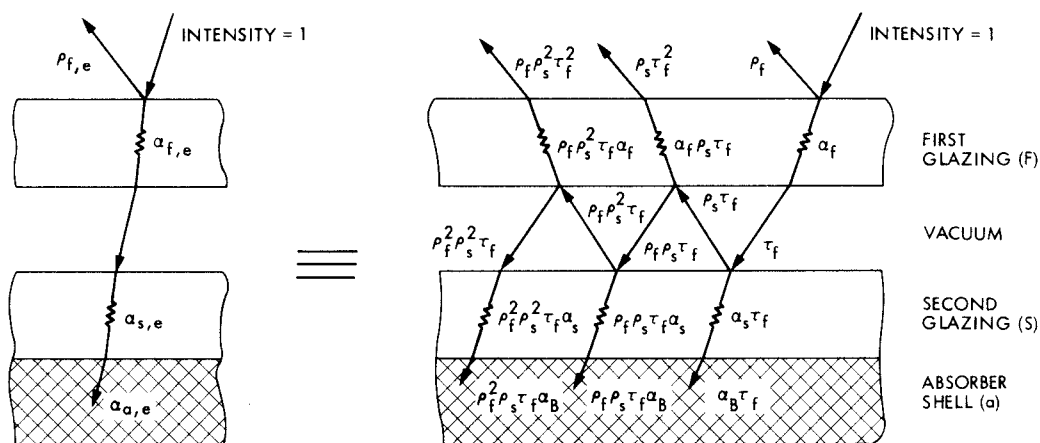


Fig. A-3. Combination of two sheets of glazing with an opaque bottom surface for the second

## Appendix B

### Derivation of Heat Transfer Rate Equations

Following the assumptions made in the Section III, a segment of the collector unit whose thickness is  $dx$  and located at a distance  $x$  from the inlet fluid section is as shown in Fig. 3. The differential rates of heat flux are divided as shown by Sankey diagram in Fig. B-1, whereby

$dQ_1$  = total solar irradiation (direct and diffuse) on the outer glass tube from all sides including the irradiation from the back V-reflector.

$$dQ_1 = \lambda ID_{f,o} dx \quad (B-1)$$

where  $\lambda$  is given by

$$\lambda = 1 + \rho_v \left( \frac{S}{D_{f,o}} - 1 \right) \quad (B-2)$$

$dQ_2$  = outward reflection loss from the collector unit

$$dQ_2 = \rho_{f,e} dQ_1 \quad (B-3)$$

where  $\rho_{f,e}$  is given by Eq. (A-10)

$dQ_3$  = effective absorbed energy by the outer glass tube

$$dQ_3 = \alpha_{f,e} dQ_1 \quad (B-4)$$

where  $\alpha_{f,e}$  is given by Eq. (A-8)

$dQ_4$  = effective absorbed energy by the second (inner) glass tube

$$dQ_4 = \alpha_{s,e} dQ_1 \quad (B-5)$$

where  $\alpha_{s,e}$  is given by Eq. (A-9)

$dQ_5$  = effective absorbed energy by the metallic absorber shell

$$dQ_5 = \alpha_{a,e} dQ_1 \quad (B-6)$$

where  $\alpha_{a,e}$  is given by Eq. (A-7)

$dQ_6$  = conduction heat transfer between the second (inner) glass tube and the absorber shell

$$dQ_6 = \frac{2\pi (T_a - T_s) dx}{\left[ \frac{\ln(D_{s,o}/D_{s,i})}{K_s} + \frac{\ln(D_{a,o}/D_{a,i})}{K_a} \right]} \quad (B-7)$$

$dQ_7$  = convection heat transfer between the absorber shell and the air trapped in the absorber core

$$dQ_7 = H_{aA} (T_a - T_A) \pi(D_{a,i} + 2D_{t,o}) dx \quad (B-8)$$

$dQ_8$  = convection heat transfer between the absorber tubes and the hot fluid

$$dQ_8 = H_{ah} (T_a - T_h) \pi D_{t,i} dx \quad (B-9)$$

$dQ_9$  = convection heat transfer between the absorber tubes and the cold fluid

$$dQ_9 = H_{ac} (T_a - T_c) \pi D_{t,i} dx \quad (B-10)$$

$dQ_{10}$  = sensible heat gain by the hot fluid

$$dQ_{10} = -\dot{m}c_p \left( \frac{dT_h}{dx} \right) dx \quad (B-11)$$

where the  $(-)$  sign was introduced since the hot fluid flow is in the opposite direction to the positive  $x$  direction.

$dQ_{11}$  = sensible heat gain by the cold fluid

$$dQ_{11} = +\dot{m}c_p \left( \frac{dT_c}{dx} \right) dx \quad (B-12)$$

$dQ_{12}$  = radiation heat transfer between the second (inner) glass tube and the first (outer) glass tube

$$dQ_{12} = \frac{\sigma (T_s^4 - T_f^4) \pi D_{s,o} dx}{\frac{1}{\epsilon_s} + \left( \frac{1}{\epsilon_f} - 1 \right) \left( \frac{D_{s,o}}{D_{f,i}} \right)} \quad (B-13)$$

$dQ_{13}$  = radiation heat losses from the outer surface of the first (outer) glass tube to the ambient air

$$dQ_{13} = \sigma \epsilon_f (T_f^4 - T_A^4) \pi D_{f,o} dx \quad (\text{B-14})$$

$dQ_{14}$  = convection heat transfer from the outer surface of the first (outer) glass tube to the ambient air

$$dQ_{14} = H_{fAm} (T_f - T_A) \pi D_{f,o} dx \quad (\text{B-15})$$

Applying the first law of thermodynamics at steady state to the collector components will yield the following heat balance equations (see Refs., 5 and 6):

For the absorber tube:

$$dQ_5 - (dQ_6 + dQ_7 + dQ_8 + dQ_9) = 0 \quad (\text{B-16})$$

For the hot fluid:

$$dQ_8 - dQ_{10} = 0 \quad (\text{B-17})$$

For the cold fluid:

$$dQ_9 - dQ_{11} = 0 \quad (\text{B-18})$$

For the first (outer) glass cover:

$$dQ_3 + dQ_{12} - dQ_{13} - dQ_{14} = 0 \quad (\text{B-19})$$

For the second (inner) glass cover:

$$dQ_4 + dQ_6 - dQ_{12} = 0 \quad (\text{B-20})$$

For the incident solar energy:

$$dQ_1 - dQ_2 - dQ_3 - dQ_4 - dQ_5 = 0 \quad (\text{B-21})$$

Summing Eqs. (B-16) through (B-21) yields

$$dQ_1 - (dQ_2 + dQ_7 + dQ_{13} + dQ_{14}) = 0 \quad (\text{B-22})$$

Equation (B-22) shows that the thermal losses from the collector will be only the summation of (1) the outward light reflection from the first (outer) glass tube, (2) the convection and radiation heat transfer to the ambient air and sky from the

first (outer) glass, and (3) the convection heat transfer from the inner absorber walls to the air core and ambient air.

The elementary radiation heat transfer  $dQ_{12}$  and  $dQ_{13}$  are further linearized by defining the radiation heat transfer coefficients  $R_{sf}$  and  $R_{fAm}$  such that

$$\left. \begin{aligned} R_{sf} &= \frac{\sigma (T_s^4 - T_f^4)}{(T_s - T_f) \left[ \frac{1}{\epsilon_s} + \left( \frac{1}{\epsilon_f} - 1 \right) \left( \frac{D_{s,o}}{D_{f,i}} \right) \right]} \\ R_{fAm} &= \epsilon_f \frac{\sigma (T_f^4 - T_A^4)}{(T_f - T_A)} \end{aligned} \right\} \quad (\text{B-23})$$

Equations (B-13) and (B-14) are reduced to

$$dQ_{12} = R_{sf} \pi D_{s,o} (T_s - T_f) dx \quad (\text{B-13})$$

$$dQ_{13} = R_{fAm} \pi D_{f,o} (T_f - T_A) dx \quad (\text{B-14})$$

The five linearized heat balance equations, Eqs. (B-16) through (B-20), will be grouped after division by  $(D_{f,o} dx)$  as follows:

For the absorber shell:

$$\begin{aligned} E_1 - B_1 (T_a - T_s) - B_2 (T_a - T_A) - B_3 (T_a - T_c) \\ - B_3 (T_a - T_h) = 0 \end{aligned} \quad (\text{B-24})$$

For the hot fluid:

$$G \frac{dT_h}{dx} = -B_3 (T_a - T_h) \quad (\text{B-25})$$

For the cold fluid:

$$G \frac{dT_c}{dx} = B_3 (T_a - T_c) \quad (\text{B-26})$$

For the first (outer) glass tube:

$$E_2 + B_4 (T_s - T_f) - B_5 (T_f - T_A) = 0 \quad (\text{B-27})$$

For the second (inner) glass tube:

$$E_3 + B_1 (T_a - T_s) - B_4 (T_s - T_f) = 0 \quad (\text{B-28})$$

where

$$\left. \begin{aligned} B_1 &= \frac{2\pi/D_{f,o}}{\left[ \frac{\ln(D_{s,o}/D_{s,i})}{K_s} + \frac{\ln(D_{a,o}/D_{a,i})}{K_a} \right]} \\ B_2 &= \pi(D_{a,i} + 2D_{t,o})H_{aA}/D_{f,o} \\ B_3 &= \pi(D_{t,i}/D_{f,o})H_{ah} \\ B_4 &= \pi R_{sf}(D_{s,o}/D_{f,o}) \\ B_5 &= \pi(H_{fAm} + R_{fAm}) \end{aligned} \right\} \quad (\text{B-29})$$

$$\left. \begin{aligned} E_1 &= \alpha_{a,e} \lambda I \\ E_2 &= \alpha_{f,e} \lambda I \\ E_3 &= \alpha_{s,e} \lambda I \\ G &= \dot{m}c_p/D_{f,o} \end{aligned} \right\} \quad (\text{B-30})$$

Expressing the temperatures  $T_f$  and  $T_s$  in terms of  $T_a$  using Eqs. (B-24), (B-27), and (B-28) yields

$$\left. \begin{aligned} T_f &= (E_4 + B_4 T_s)/B_6 \\ T_s &= (E_5 + B_6 T_a)/B_7 \\ T_a &= [E_6 + B_3 (T_h + T_c)]/B_8 \end{aligned} \right\} \quad (\text{B-31})$$

where

$$\left. \begin{aligned} E_4 &= E_2 + B_5 T_A, \quad B_6 = (B_4 + B_5) \\ E_5 &= E_3 \frac{B_6}{B_1} + E_4 \frac{B_4}{B_1}, \quad B_7 = B_6 + \frac{B_4 B_5}{B_1} \\ E_6 &= E_1 + B_2 T_A + \frac{B_1 E_5}{B_7}, \quad B_8 = B_2 + 2B_3 + \frac{B_4 B_5}{B_7} \end{aligned} \right\} \quad (\text{B-32})$$

Substituting in Eqs. (B-25) and (B-26), the two differential equations for the hot and cold fluid streams at any position  $X$  will be

$$\frac{dT_h}{dx} = -\delta - C_0 T_c + C_1 T_h \quad (\text{B-33})$$

and

$$\frac{dT_c}{dx} = \delta + C_0 T_h - C_1 T_c \quad (\text{B-34})$$

where

$$\left. \begin{aligned} \delta &= \frac{B_3}{B_8}, \quad \frac{E_6}{G} \\ C_0 &= \frac{B_3^2}{GB_8} \\ C_1 &= \frac{B_3}{GB_8} (B_8 - B_3) \end{aligned} \right\} \quad (\text{B-35})$$

The term  $\delta/(C_1 - C_0)$  appears in solving Eqs. (B-33) and (B-34) and can be expressed as:

$$\frac{\delta}{(C_1 - C_0)} = T_A + \frac{\left( E_1 + E_2 \frac{B_4}{B_7} + E_3 \frac{B_6}{B_7} \right)}{\left( B_2 + \frac{B_4 B_5}{B_7} \right)} \quad (\text{B-36})$$

The overall heat loss coefficient  $B_0$  follows from Eq. (B-36), to be

$$B_0 = \left( B_2 + \frac{B_4 B_5}{B_7} \right) \quad (\text{B-37})$$

Eqs. (B-36) and (B-37) are useful in giving the physical meaning needed to the collector efficiency expression as shown in the text.

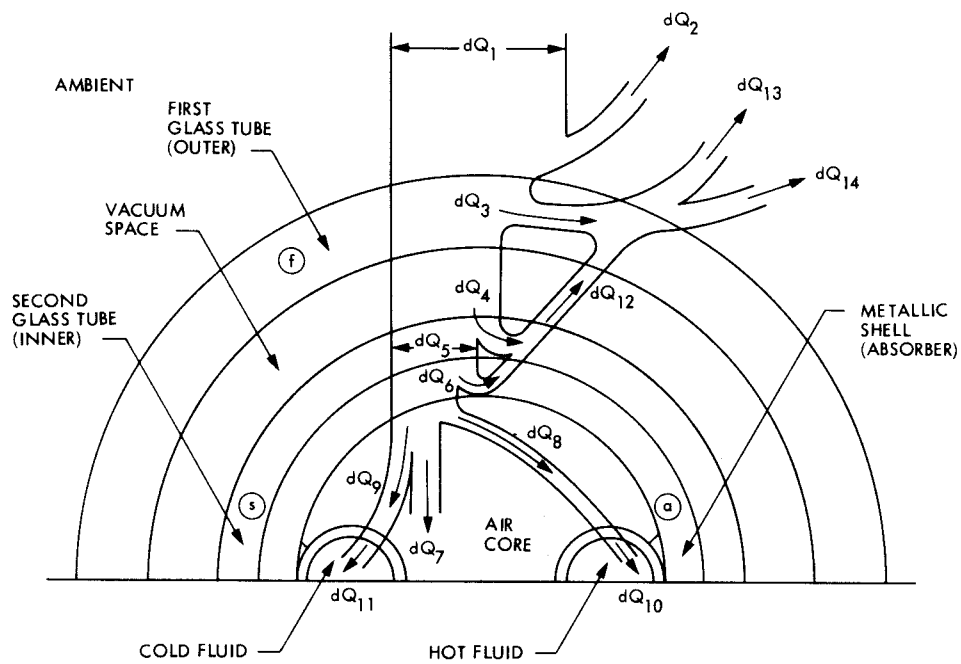


Fig. B-1. Sankey diagram for tubular collector